Electronic Supplementary Information

Ultrathin metal−organic layers/carbon nitride nanosheet composites as 2D/2D heterojunctions for efficient CO_2 photoreduction

Wei Yang,[a,b†] Xiao Lin,[a†] Wen-Jie Shi,[a†] Ji-Hong Zhang,[a] Yu-Chen Wang,[a] Ji-Hua Deng,[a*] Di-Chang Zhong[a*] and Tong-Bu Lu[a*]

[a] *Institute for New Energy Materials & Low Carbon Technologies, School of Material Science & Engineering, School of Chemistry & Chemical Engineering, Tianjin University of Technology, Tianjin 300384, China*

[b] *Institute of Coal Chemistry, State Key Laboratory of Coal Conversion, Chinese Academy of Sciences, Taiyuan 030001, China*

[†] These authors contributed equally to this work.

[*] Corresponding authors:

E-mail: djhycu_2006@aliyun.com (J. H. Deng);

E-mail: dczhong@email.tjut.edu.cn (D. C. Zhong);

E-mail: lutongbu@tjut.edu.cn (T. B. Lu).

1. Materials and methods

1.1 Materials

All chemicals and materials were commercially obtained and used without any further purification. Nafion solution (5 wt%) was purchased from Alfa Aesar. All solutions used in electrochemical experiments were prepared with Millipore water (18.2 MΩ). The purity of Argon is 99.999%.

1.2 Preparation

Synthesis of Co-MOF

Bulk Co-MOF was prepared by the hydrothermal method.[1] H_2BDC (24.9 mg, 0.15 mmol) and $Co(NO_3)_2 \cdot H_2O$ (43.7 mg, 0.15 mmol) were dissolved in 7.2 mL DMF/H_2O/ethanol (16:1:1) mixed solution under ultrasonication. Then the mixed solution was transferred into a 20 mL Teflon-lined stainless-steel autoclave and heated at 140 ºC for 48 h. After cooling down to the room temperature, the received product was collected via filtration and washed with H_2O and EtOH by several times. The final product was dried at 50 ºC in a vacuum oven for 12 h.

Synthesis of Co-MOF/CN(400) nanocomposites

g-C_3N_4 powder (400 mg) and $Co(NO_3)_2 \cdot H_2O$ (43.7 mg, 0.15 mmol) were dispersed in 7.2 mL DMF/H_2O/ethanol (16:1:1) mixed solvent with ultrasonication for 1h. 0.15 mmol H_2BDC was dissolved in the solution and stirred for 0.5 h. Afterward, we transferred the mixed solution into a 20 mL Teflon-lined stainless-steel autoclave and heated it at 140 ºC for 48 h. The received product was collected via filtration and washed with H_2O and EtOH by several times. The final product was dried at 50 ºC in a vacuum oven for 12 h.

Synthesis of Fe-MOL/CN(400), Ni-MOL/CN(400), and Cu-MOL/CN(400) nanocomposites

The Fe-MOL/CN(400), Ni-MOL/CN(400), and Cu-MOL/CN(400) nanocomposites were prepared with a similar procedure to Co-MOL/CN(400) except using other metal salts instead of $Co(NO_3)_2 \cdot H_2O$.

1.3 Methods

The X-ray powder diffraction (XRD) of all the materials were recorded on a Smart X-ray diffractometer (SmartLab 9 KW, Rigaku, apan) equipped with graphite monochromatized with Cu Kα source (radiation) (λ = 1.54178 Å). Fourier transform infrared (FT-IR) spectra were recorded on a Perkin Elmer Frontier Mid-IR FTIR spectrometer in the 400-4000 cm^{-1} region with KBr pellets. A CO_2 sorption test was performed on a multi-station specific surface micropore, and vapor adsorption analyzer (BELSORP-Mas, MicrotracBEL, Japan) at 298 K. X-ray photoelectron spectra (XPS) were conducted on ESCA LAB 250 Xi spectrometer (Thermo Scientific, USA) with Al Kα as the excitation source. The solid-state UV-Vis absorption spectrum was obtained by a UV-vis spectrophotometer (UV-3600, Shimadzu, Japan). Scanning electron microscope (SEM) images were recorded on a Verios 460 L Ultrahigh Resolution Scanning Electron Microscope. The transmission electron microscopy (TEM) was carried out using a Tecnai G2 Spirit TWIN at an acceleration voltage of 120 KV. HAADF images and Energy-dispersive X-ray spectroscopy (EDS) were taken using High-Resolution Transmission Electron Microscope EFG (Talos F200 X, FEI, USA). Atomic force microscopy (AFM) images were recorded on a Bruker Icon (America) scanning probe microscope in tapping mode in the air. The metal (Co) contents in prepared catalysts were measured by inductively coupled plasma-atomic emission spectroscopy (ICP-AES, SPECTRO BLUE). Electrochemical measurements were carried out on a CHI 670E electrochemical workstation. The photoluminescence (PL) spectra were conducted on a fluorescence spectrophotometer (F-7000, Hitachi, Japan), and the experimental data were analyzed by the SymPhoTime 64. Time-resolved fluorescence (TRF) spectra were tested by another fluorescence spectrophotometer (Horiba FL-3, HORIBA Scientific, USA). The isotopic labeling experiment was conducted under a $^{13}CO_2$ atmosphere, and the gas products were analyzed by a quantitative mass spectrometer (HPR-20 Q/C Benchtop

Gas Analysis System). The evolved CO and H_2 were monitored using an Agilent 7820A gas chromatography equipped with two automated gas sampling valves containing a thermal conductivity detector (TCD) and a flame ionization detector (FID).

AFM Measurements. 0.5 mg of Co-MOLs or Co-MOLs/CN was dispersed in 1 mL ethanol, followed by ultrasonication (40 KHz) for 1 h, resulting in a suspension, which was then dropped (~20 μL) onto a clean mica sheet. The supported sample was dried at room temperature for 4 h and used for AFM measurements.

ICP-MS Measurements. 1 mg of Co-MOLs/CN(x) was suspended in nitric acid (14.4 M, 5 mL, GR). The mixture was ultrasonicated continuously for 2–3 min to form a uniform suspension. The suspension was subjected to microwave treatment at 80 °C for 20 min. After that, the mixture was centrifuged at 10000 rpm. 250 μL of the supernatant was diluted to 10 mL by adding deionized water. Three parallel measurements were carried out for each sample, and average value was reported.

CO_2 Sorption. CO_2 sorption measurements for CN, Co-MOF, Co-MOL, or Co-MOF/CN(400) or Co-MOL/CN(400) were performed on a BELSORP-max automatic volumetric adsorption apparatus. The constant temperature of 298 K were controlled by circulating water bath. The adsorption isotherms were collected in a relative pressure range from 10^{-4} to 1.0 atm. The initial outgassing process for all samples was carried out under a high vacuum (less than 10^{-6} mbar) at 120 °C for 10 h. The degassed sample and sample tubes were weighed precisely and transferred to the analyser.

2. Photocatalytic CO_2 reduction test

The photocatalytic CO_2 reduction experiments were performed on a 17 mL reactor containing the catalyst, 2,2'-dipyridine, 3 mL of DI-water, 1 mL CH_3CN and 1 mL TEOA at ambient temperature and atmospheric pressure. After the reaction system was purged with CO_2 for 30 min, the photocatalytic reaction was initiated by irradiation under a Xe lamp with a UV-cutoff filter (300 mW, $\lambda \geq 420$ nm). A gas chromatography analyzed the generated gases in the headspace. Each photocatalytic reaction was repeated at least three times to confirm the reliability of the data. Recycling experiments were carried out under similar conditions using the collected catalyst after the photocatalytic test instead of fresh motivation.

3. Electrochemical and photoelectrochemical tests

All electrochemical measurements were conducted in an airtight cell using a CHI 670E Potentiostate with a three-electrode configuration. Platinum foil and an Ag/AgCl (3 M KCl) electrode were used as counter and reference electrodes, respectively. To prepare the working electrode, 5 mg of the catalyst was dispersed in ethanol solvent (1 mL) with 50 μL Nafion solution (5 wt% in water). Then, the suspension was ultrasonicated for 30 min to generate a homogeneous ink. Next, the catalyst ink (100 μL) was drop-casted onto the FTO glass with a size of 0.5 cm×2.0 cm with a 0.25 mg cm^{-2} loading for catalysts and painted onto the FTO glass with 0.5 cm×1 cm was used as the working electrode.

The electrolyte was a 0.2 M Na_2SO_4 aqueous solution saturated with Ar (pH ~7.2). Before the tests, the electrolyte was purged with Ar for at least 20 min. The Mott-Schottky curves were taken at potential ranging from −1.2 to 0.2 V (vs. Ag/AgCl) under the dark condition with different frequencies. Electrochemical impedance spectroscopy (EIS) plots were performed at potential -0.9 V vs. Ag/AgCl, with the frequency ranging from 100 kHz to 0.1 Hz and the modulation amplitude of 5 mV. The transient photocurrent measurements (TPC) were recorded at an applied potential of 0 V vs. Ag/AgCl under the visible light illumination ($\lambda \geq 420$ nm).

4. ESI tables and figures

Table S1 The percentage of Co measured by inductively coupled plasma-mass spectroscopy for different catalysts.

Materials	Co content wt%
Co-MOL	37.2057
Co-MOL/CN(100)	7.8801
Co-MOL/CN(200)	4.0059
Co-MOL/CN(300)	3.0941
Co-MOL/CN(400)	2.3633
Co-MOL/CN(500)	1.7032
Co-MOL/CN(600)	1.2775
Co-MOL/CN(800)	0.7535
CN	0

Table S2 Comparison of reported MOF-based catalysts for photocatalytic CO_2 reduction.

Entry	Photocatalyst	Solvent	Light source	Main Products ($\mu mol \cdot g^{-1} \cdot h^{-1}$)	Refs.
1	UiO-66/CNNS	MeCN/TEOA = 4:1	300 W Xe-lamp $\lambda \geq 420$ nm	CO (9.9)	[2]
2	BIF-20@ g-C_3N_4	MeCN/TEOA = 4:1	300 W Xe-lamp	CO (53.9) CH_4 (15.5)	[3]
3	NUZ/HGN-35%	TEOA/H_2O = 20:1	300 W Xe-lamp	CO (31.6)	[4]
4	4NiMOF/CN-AA	H_2O	300 W Xe-lamp $\lambda \geq 420$ nm	CO+CH_4 (54.5)	[5]
5	TiO–CN	MeCN/TEOA/H_2O = 3:1:1	300 W Xe lamp $\lambda \geq 420$ nm	CO (283.9)	[6]
6	Co-ZIF-9/g-C_3N_4	MeCN/TEOA/H_2O = 3:2:1	300 W Xe lamp $\lambda \geq 420$ nm	CO (10.4)	[7]
7	g-C_3N_4-MOLs-30	MeCN/TEOA/H_2O = 3:1:1	300 W Xe lamp $\lambda \geq 420$ nm	CO (464.1)	[8]
8	TCNZ8	H_2SO_4 (0.3 mL, 2 M) $NaHCO_3$ (84 mg)	300 W Xe lamp	CH_3OH (0.75)	[9]
9	CoMOL/CN(400)	MeCN/TEOA/H_2O = 3:1:1	300 W Xe lamp $\lambda \geq 420$ nm	CO (539.1)	**This Work**

Table S3 Multiexponential fit parameters for the decay of photoluminescence lifetime (Excitation wavelength: 365 nm; Detection wavelength: 545 nm).

	τ_1	τ_2	τ_3	Average lifetime $< \tau_{ave} >$ (ns)
CN	1.11	1.11	4.58	1.96
A	47.78	27.60	24.62	
CN/ FLNMF	1.03	1.03	4.09	1.83
A	44.21	29.47	26.32	

An $A_1+A_2+A_3=1$; The calculation formula of average lifetime $\tau_{Ave} = \sum \tau_i * A_i$.

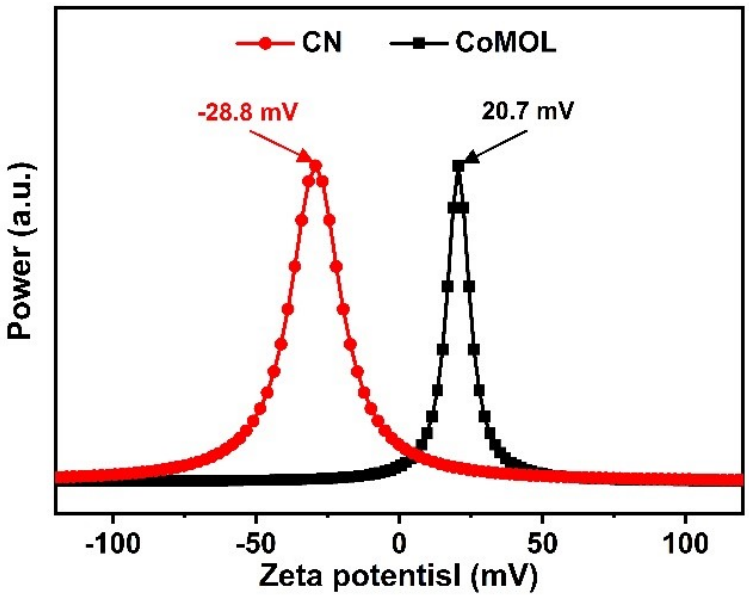

Fig. S1 Zeta potential of CN and Co-MOL dispersed in deionized water.

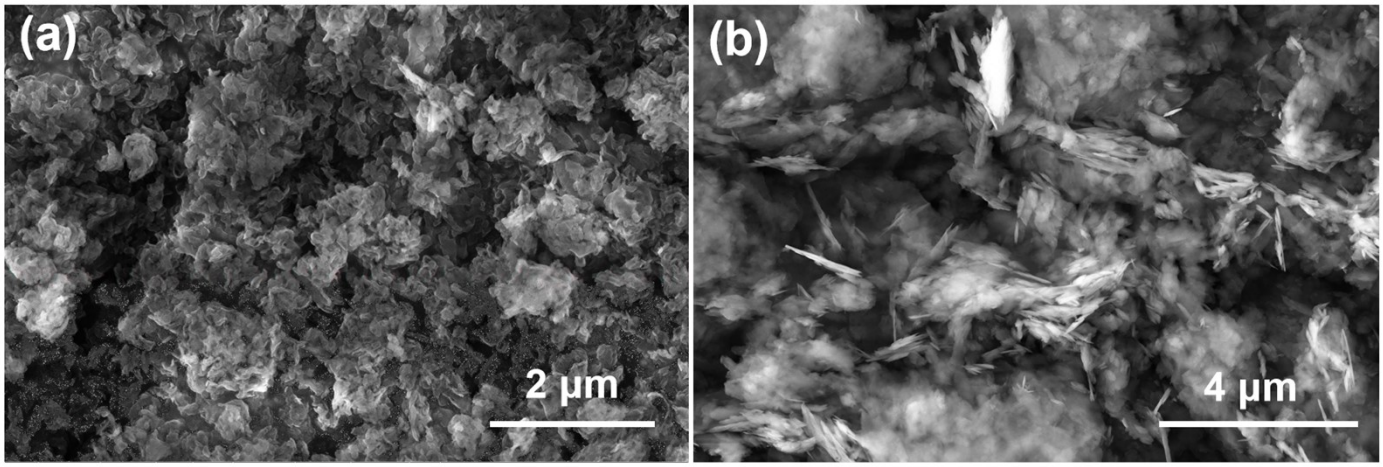

Fig. S2 HRSEM images of CN (a) and Co-MOL (b).

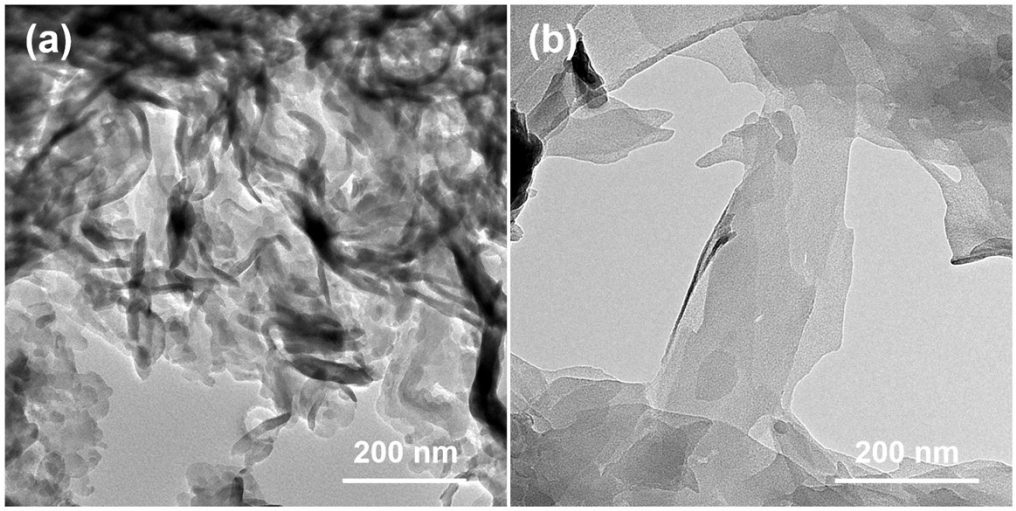

Fig. S3 TEM images of CN (a) and Co-MOL (b).

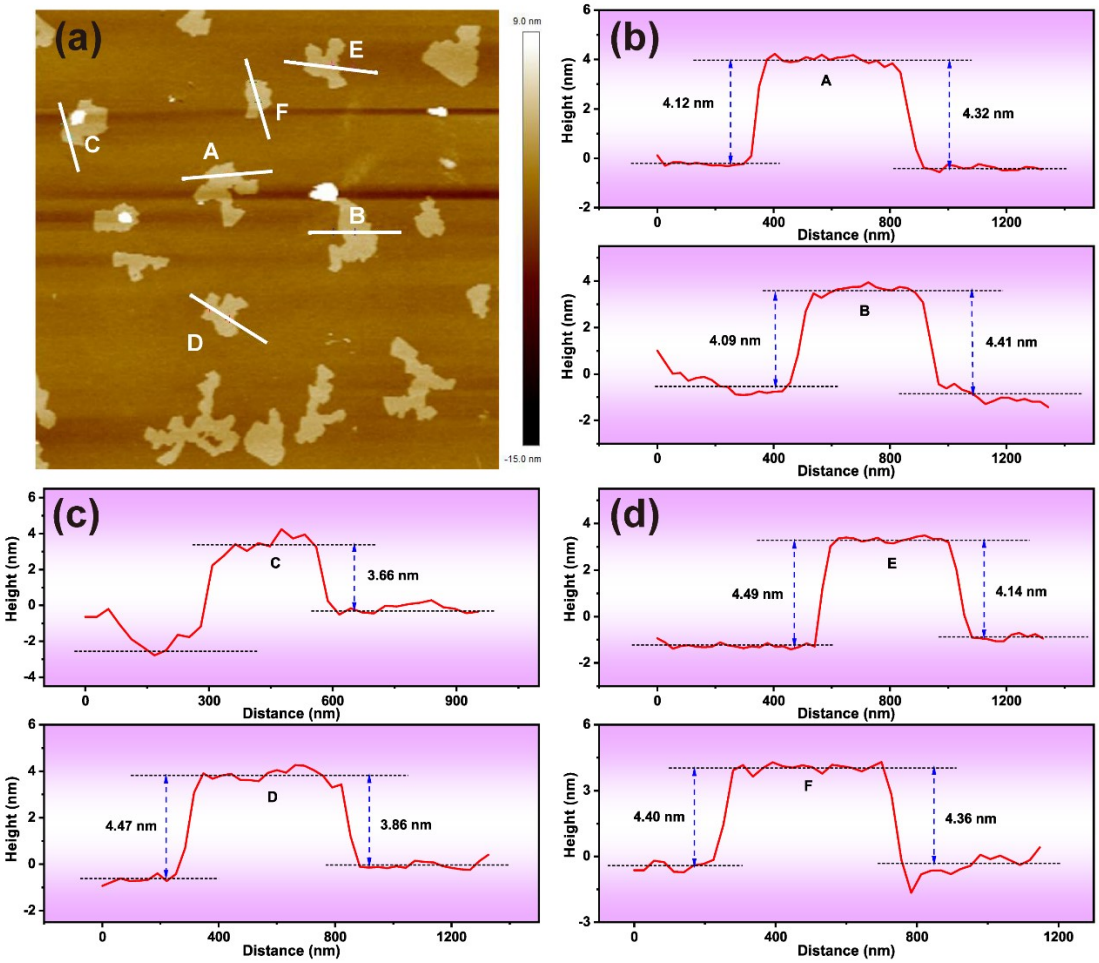

Fig. S4 (a) AFM images of Co-MOL, and (b-d) the corresponding height profiles.

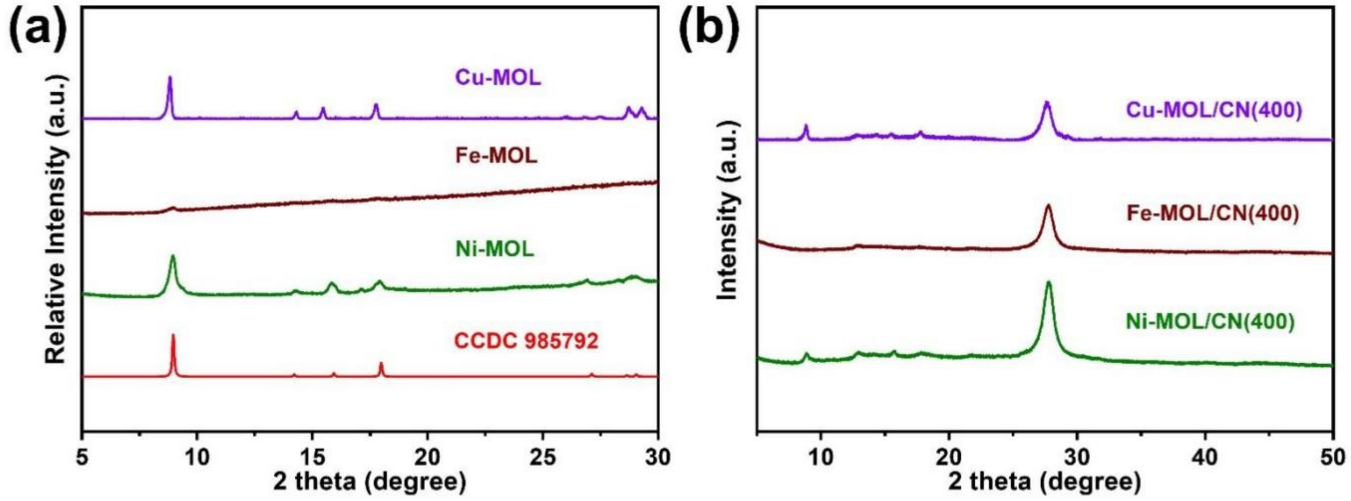

Fig. S5 (a) XRD patterns for M-MOL (M = Cu, Fe and Ni) and (b) M-MOL/CN(400) (M = Cu, Fe and Ni).

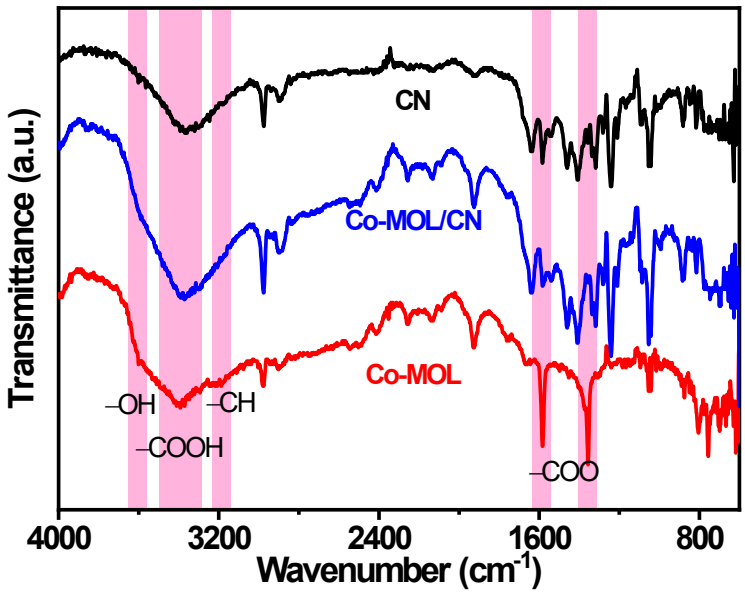

Fig. S6 FT-IR spectra of Co-MOL (red), CN (black), and Co-MOL/CN(400) (blue).

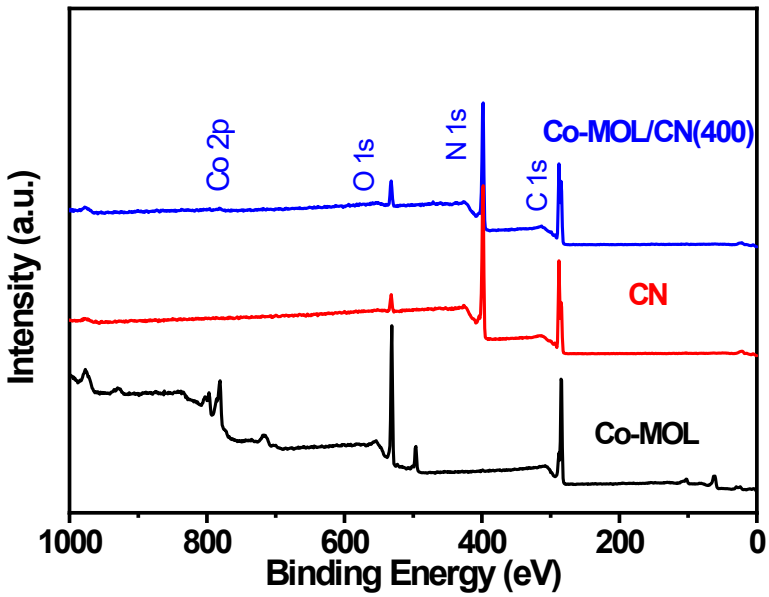

Fig. S7 XPS survey spectrum of the Co-MOL (black), CN (red) , and Co-MOL/CN(400) (blue).

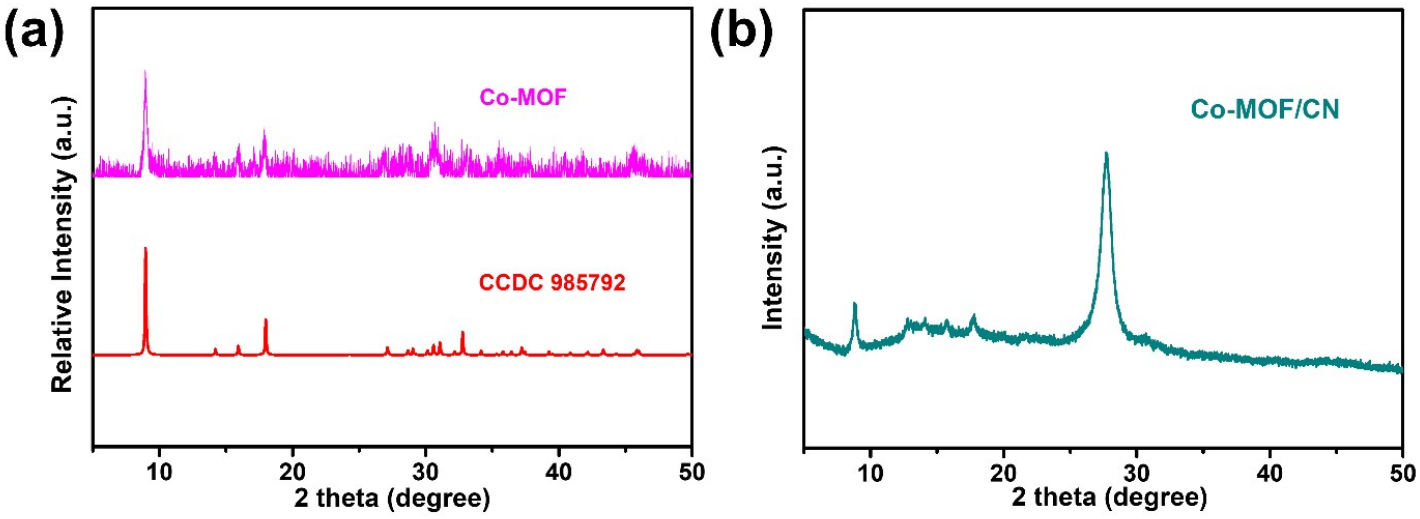

Fig. S8 Powder XRD patterns for (a) MOF and (b) Co-MOF/CN(400).

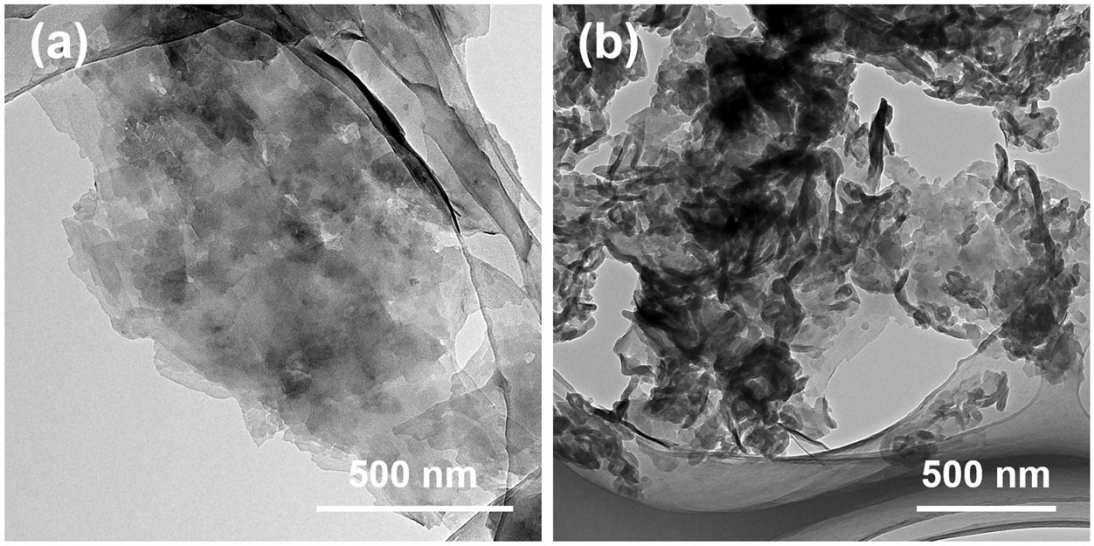

Fig. S9 (a) TEM images of Co-MOF and (b) Co-MOF/CN.

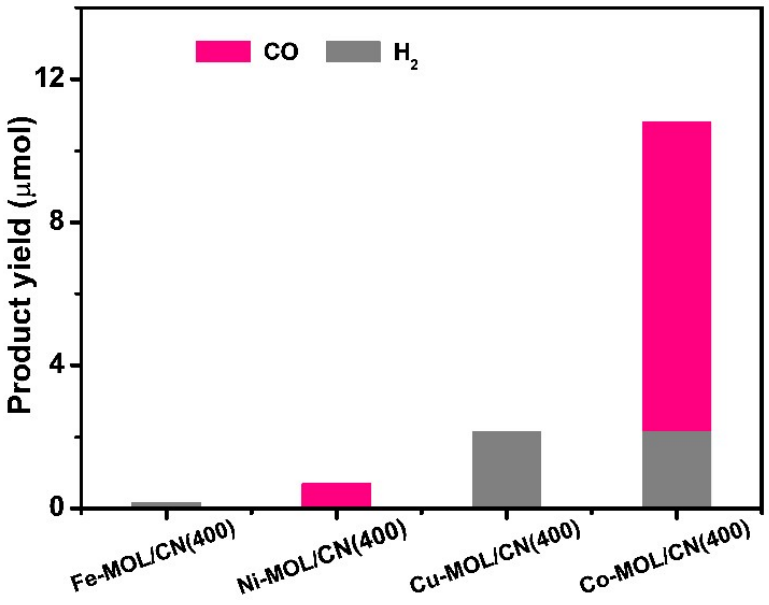

Fig. S10 CO_2 photoreduction performance for Fe-MOL/CN(400), Ni-MOL/CN(400), and Cu-MOL/CN(400) , Co-MOL/CN(400).

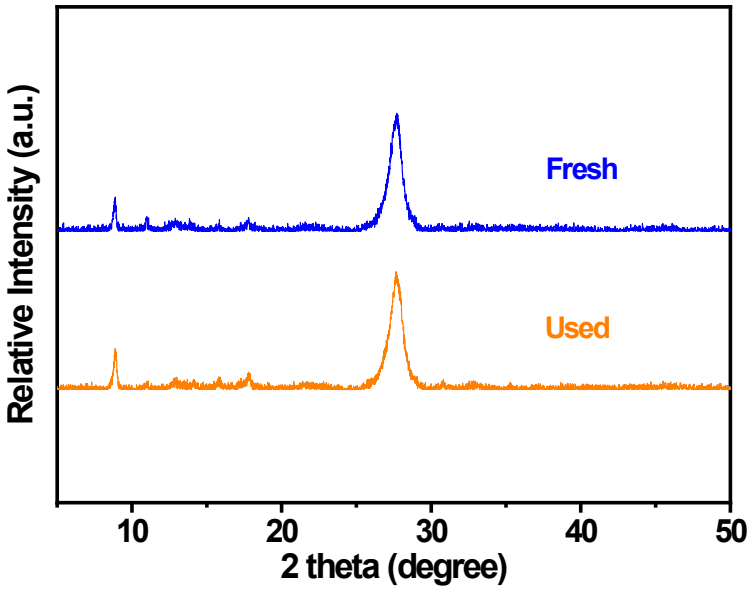

Fig. S11 Powder XRD spectra for fresh and used Co-MOL/CN(400).

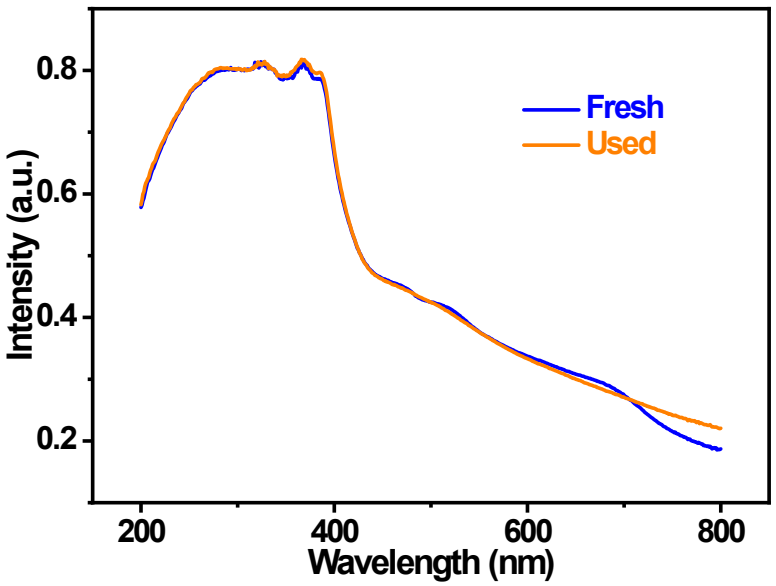

Fig. S12 UV–vis spectra for Co-MOL/CN(400) before and after reaction.

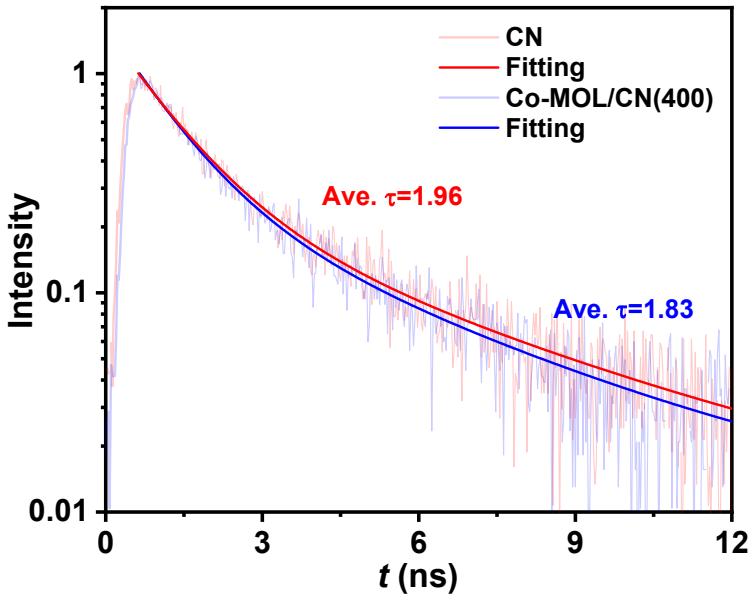

Fig. S13 PL decay curves of CN and Co-MOL/CN(400) (Excitation wavelength: 380 nm; Detection wavelength: 436 nm).

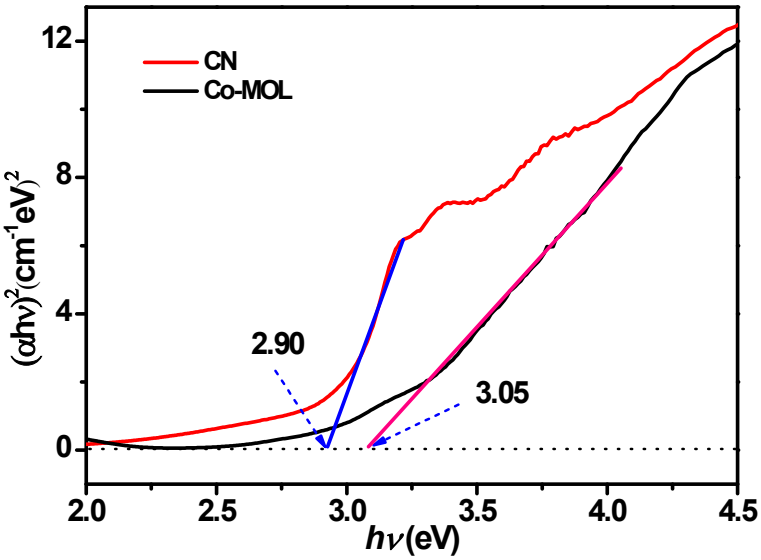

Fig. S14 The corresponding Tauc plots of $(\alpha h\upsilon)^2$ versus hν of CN and Co-MOL.

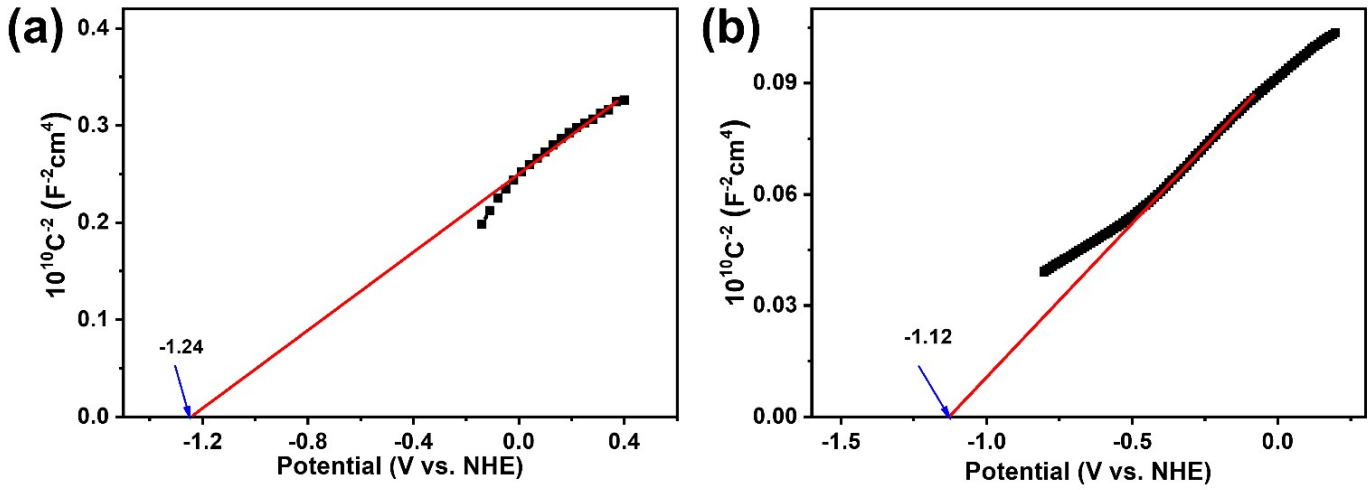

Fig. S15 Mott-Schottky plots of (a) CN and (b) Co-MOL at frequencies 1.0 kHz.

Reference

[1] A. Mesbah, P. Rabu, R.M. Sibille, S. Lebègue, T.M. Mazet, B.N. Malaman, and M. François, From Hydrated $Ni_3(OH)_2(C_8H_4O_4)_2(H_2O)_4$ to Anhydrous $Ni_2(OH)_2(C_8H_4O_4)$: Impact of Structural Transformations on Magnetic Properties, *Inorg. Chem.*, **2014**, 53, 872-881.

[2] L. Shi, T. Wang, H. Zhang, K. Chang, J. Ye, Electrostatic Self-Assembly of Nanosized Carbon Nitride Nanosheet onto a Zirconium Metal–Organic Framework for Enhanced Photocatalytic CO_2 Reduction, *Adv. Funct. Mater.*, **2015**, 25, 5360-5367.

[3] G. Xu, H. Zhang, J. Wei, H.-X. Zhang, X. Wu, Y. Li, C. Li, J. Zhang, J. Ye, Integrating the g-C_3N_4 Nanosheet with B–H Bonding Decorated Metal–Organic Framework for CO_2 Activation and Photoreduction, *ACS Nano*, **2018**, 12, 5333-5340.

[4] Y. Wang, L. Guo, Y. Zeng, H. Guo, S. Wan, M. Ou, S. Zhang, Q. Zhong, Amino-Assisted NH_2-UiO-66 Anchored on Porous g-C_3N_4 for Enhanced Visible-Light-Driven CO_2 Reduction, *ACS Appl. Mater. Interfaces*, **2019**, 11, 30673-30681. ACS Appl Mater Interfaces

[5] L. Zhao, Z. Zhao, Y. Li, X. Chu, Z. Li, Y. Qu, L. Bai, L. Jing, The synthesis of interface-modulated ultrathin Ni(ii) MOF/g-C_3N_4 heterojunctions as efficient photocatalysts for CO_2 reduction, *Nanoscale*, **2020**, 12, 10010-10018.

[6] S. Tang, X. Yin, G. Wang, X. Lu, T. Lu, Single titanium-oxide species implanted in 2D g-C_3N_4 matrix as a highly efficient visible-light CO_2 reduction photocatalyst, *Nano Res.,* **2019**, 12, 457-462.

[7] S. Wang, J. Lin, X. Wang, Semiconductor–redox catalysis promoted by metal–organic frameworks for CO_2 reduction, *Phys. Chem. Chem. Phys.*, **2014**, 16, 14656-14660.

[8] J.-H. Zhang, W. Yang, M. Zhang, H.-J. Wang, R. Si, D.-C. Zhong, T.-B. Lu, Metal-organic layers as a platform for developing single-atom catalysts for photochemical CO_2 reduction, *Nano Energy.*, **2021**, 80, 105542.

[9] S. Liu, F. Chen, S. Li, X. Peng, Y. Xiong, Enhanced photocatalytic conversion of greenhouse gas CO_2 into solar fuels over g-C_3N_4 nanotubes with decorated transparent ZIF-8 nanoclusters, *Appl. Catal. B,* **2017**, 211, 1-10.